PNAS
www.pnas.org

Supplementary Information for:

mGreenLantern: a bright monomeric fluorescent protein with rapid expression and cell filling properties for neuronal imaging

Benjamin C. Campbell, Elisa M. Nabel, Mitchell H. Murdock, Cristina Lao-Peregrin, Pantelis Tsoulfas, Murray G. Blackmore, Francis S. Lee, Conor Liston, Hirofumi Morishita, Gregory A. Petsko

Benjamin C. Campbell
Email: bec2017@med.cornell.edu

Gregory A. Petsko
Email: gpetsko@med.cornell.edu

This PDF file includes:

Supplementary text
Figures S1 to S11
Tables S1 to S4
Legend for Movie S1
SI References

Other supplementary materials for this manuscript include the following:

Movie S1

Materials and Methods

Plasmid construction and cloning

All FPs for bacterial expression were cloned using isothermal assembly (1) into a modified pBAD/His-B vector (Invitrogen) featuring a shortened N-terminal His_6 tag, MGSHHHHHHGRS, originating from Addgene #37129 (2). EYFP and mNeonGreen were synthesized (Eurofins Genomics) using sequences from pAAV-Ef1a-DIO-EYFP (Addgene #27056) and GenBank KC295282, respectively. A list of plasmid backbones used for construction of targeting vectors in this study can be found in **SI Appendix, Table 4** with the accompanying citations.

pcDNA3.1-4mt-mGreenLantern was produced by PCR-amplifying the quadruplicate COX8A mitochondrial targeting sequence "4mt" from pcDNA-4mtD3cpv (Addgene #36324) and cloning it N-terminal to the insert into a linearized pcDNA3.1-mGreenLantern plasmid using isothermal assembly.

pcDNA3.1-ER-mGreenLantern was constructed by circular polymerase extension cloning (CPEC) (3) of three PCR-amplified DNA fragments. Amplification efficiency and specificity was greatly facilitated by the Touchdown PCR method (4). Two fragments of the pcDNA3.1-mGreenLantern plasmid were amplified across the ampicillin resistance gene, with one end gaining the calreticulin ER-targeting sequence MLLSVPLLLGLLGLAAAD by oligonucleotide overhangs (N-terminal to the FP insert), and the second gaining the KDEL retention sequence (C-terminal to the FP insert) followed by a stop codon. The mGreenLantern insert was amplified without its stop codon using oligonucleotides supplying site-specific overhangs for the calreticulin- and KDEL-containing plasmid backbone. These three fragments were assembled into a circular plasmid using CPEC.

pcDNA3.1-[FP]-P2A-mCherry for cytosolic co-expression of two FPs was constructed using isothermal assembly of three PCR-amplified DNA fragments: 1) P2A-mCherry sequence was amplified from AmCyan-P2A-mCherry (Addgene #45350); 2) an empty pcDNA3.1 vector was linearized at the MCS; 3) The EGFP gene was amplified with overhangs compatible for the vector and P2A-mCherry fragments. Successful clones were identified by sequencing (Macrogen). No restriction sites were modified. Subsequent cloning into this vector was performed using restriction digestion between the *EcoRI/Esp3I* sites, or by site-directed mutagenesis to derive point mutants.

Site-directed mutagenesis

Site-directed mutagenesis was performed using the QuikChange (Stratagene) method with *Pfu* polymerase (Agilent), or using the QuikChange Lightning Multi Site-Directed Mutagenesis Kit (Agilent). *DpnI* digested reaction products were transformed into TOP10 chemically competent *E. coli* (Invitrogen, #C4040-10) and plated on LB agar containing 100 µg/mL carbenicillin and 0.02% arabinose. After 14-18 hr growth at 37 °C, colonies were promptly screened by eye using amber viewing glasses and 470 nm excitation from an E-Gel Safe Imager Blue Light Transilluminator (Invitrogen). All plasmids were confirmed by sequencing (Macrogen). All oligonucleotides used in this study were produced by Eurofins Genomics.

Chromophore maturation in bacterial lysate

Maturation assays were performed using bacterial lysate as described (5), except that TOP10 competent cells were used. Protein expression was induced with the tubes filled to the brim and sealed tightly to restrict oxygen. Triplicate experiments were averaged.

Protein purification and spectroscopy

Fluorescent protein expression was induced by growing 50-500 mL TOP10 cultures in LB with ampicillin (100 µg/mL) to $OD_{600} \approx 0.6$, adding arabinose to 0.2% final concentration, and continuing growth at 37 °C for 24 hr with 275 rpm shaking. Bacteria were then pelleted, freeze-thawed, resuspended in PBS supplemented with lysozyme, and sonicated in an ice-water bath. Protein was isolated from clarified lysate after centrifugation, using HisPur Ni-NTA resin (Thermo Scientific) according to manufacturer instructions. Purified protein was dialyzed into PBS overnight, concentrated using Amicon centrifugal filter units if necessary (EMD-Millpore), and flash frozen in PBS supplemented with 10% glycerol, using liquid nitrogen.

Quantum yield and extinction coefficients were determined as described (5). pK_a values were determined as described (6). Gel filtration chromatography was performed using a Superdex 200 Increase 10/300 GL (GE Healthcare), with purified proteins loaded at the indicated concentrations in 500 µL vol and eluted at a flow rate of 0.35 mL/min with absorbance monitored at 280 nm.

Whole brain tissue clearing

Maturation assays were performed using bacterial lysate as described (5), except that TOP10 competent cells were used. Protein expression was induced with the tubes filled to the brim and sealed tightly to restrict oxygen. Triplicate experiments were averaged.

Plasmid construction and cloning

pAAV-CAG-H2B-mGreenLantern was constructed first by generating a synthetic cDNA optimized to the Human codon usage. The rat amino acid sequence H2B/Histone H2B type 1-C/E/G (accession #NP_001100822) was fused in frame to mGreenLantern with a linker of 8 amino acids (PPAGSPPA) between H2B and mGreenLantern. The cDNA was cloned into pAAV-CAG-GFP (Addgene #37825) by substituting the GFP with mGreenLantern using restriction enzymes BamHI and XhoI.

Viral vectors

rAAV2-retro-H2B-mGreenLantern was produced at the University of Miami, viral core facility, titer = $1.4x10^{13}$ particles/mL. Virus was concentrated and resuspended in sterile HBSS and used without further dilution.

Spinal cord surgery

All animal procedures were approved by the Marquette University Institutional Animal Care and Use Committee and complied with the National Institutes of Health Guide for the Care and Use of Laboratory Animals. Adult female C57BL/6 mice (>8 weeks old, 20–22 g) were anesthetized by ketamine/xylazine and the cervical spinal column exposed by incision of the skin and blunt dissection of muscles. Mice were mounted in a custom spine stabilizer. One microliter of rAAV2-retro particles was injected into the spinal cord through a pulled glass micropipette fitted to a 10 µL Hamilton syringe driven by a Stoelting QSI pump (catalog #53311) and guided by a

micromanipulator (pumping rate: 0.04 µL/min). AAV/CTB mixtures were injected between C4 and C5 vertebrae, unilateral injections at the same location, 0.35 mm lateral to the midline, and to depths of 0.6 and 0.8 mm.

Tissue clearing and imaging

After 2 wk expression, animals underwent transcardial perfusion with 0.9% saline and 4% paraformaldehyde solutions in 1×-PBS (15710, Electron Microscopy Sciences). Whole brains and spinal cords were dissected and fixed overnight in 4% paraformaldehyde at 4°C and washed three times in PBS pH 7.4, followed by storage in PBS. The dura was carefully and completely removed as residual dura can trap bubbles that prevent effective light-sheet microscopy. Samples were incubated on a shaker at room temperature in 50, 80, and 100% peroxide-free tetrahydrofuran (THF; Sigma-Aldrich, 401757) for 12 hr each. Peroxides were removed from THF by passing 100% THF through a chromatography column filled with basic activated aluminum oxide (Sigma-Aldrich, 199443) as previously described (7, 8). The next day, samples were transferred to BABB solution (1:2 ratio of benzyl alcohol, Sigma-Aldrich, 305197; and benzyl benzoate, Sigma-Aldrich, B6630) for at least 3 hr.

After clearing, samples were imaged within 48 hr by light-sheet microscopy (Ultramicroscope, LaVision BioTec). The ultramicroscope uses a fluorescence macro zoom microscope (Olympus MVX10) with a 2× Plan Apochromatic zoom objective (NA 0.50). Image analysis and 3D reconstructions were performed using Imaris v9.5 software (Bitplane) after removing autofluorescence using the Imaris Background Subtraction function with the default filter width so that only broad intensity variations were eliminated. Artifacts and nonspecific fluorescence surrounding the brain were segmented and removed using the automatic isosurface creation wizard based upon absolute intensity. Movies were generated using Imaris.

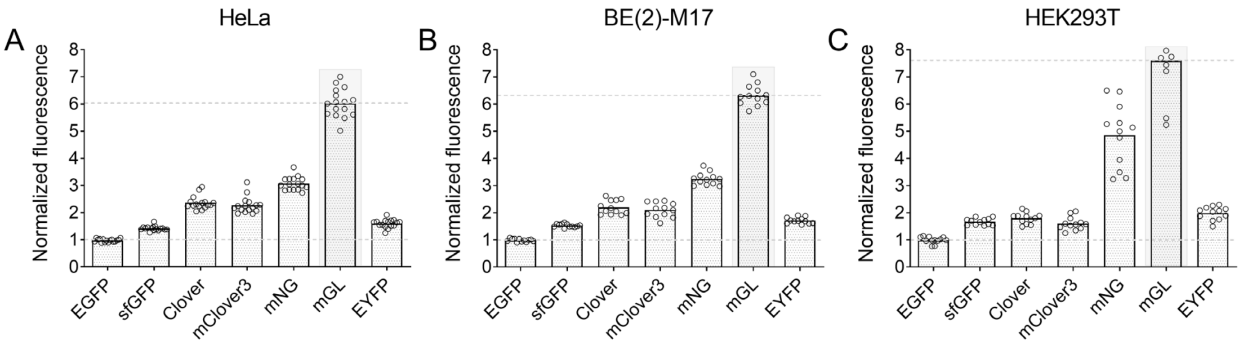

Fig. S1. Brightness of cells expressing FPs was consistent across three common mammalian cell lines. *(A*) HeLa cervical carcinoma cells, *(B*) BE(2)-M17 neuroblastoma cells, *(C)* HEK293T transformed human embryonic kidney cells. The HeLa cell figure here is identical to that in Fig. 1A to facilitate comparison between cell lines. The quantitative co-expression strategy with [FP] and mCherry ratio is used for each of the three cell types.

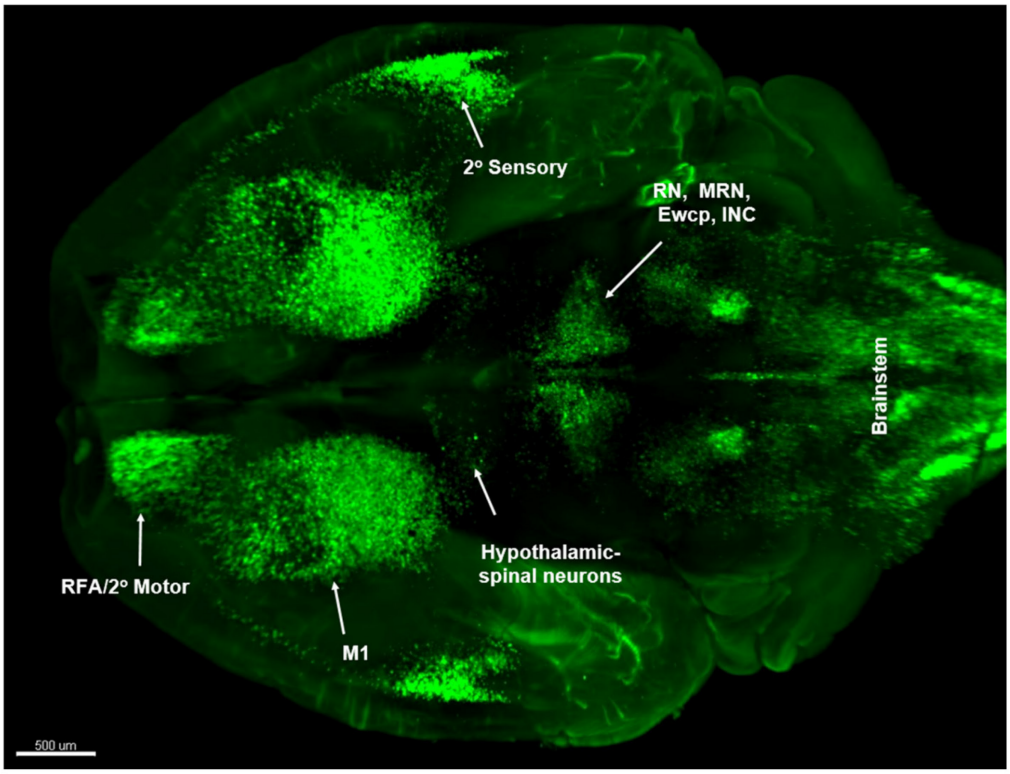

Fig. S2. 3D imaging of mGreenLantern-expressing neurons after tissue clearing reveal the distribution of nuclei of supraspinal neurons. Adult mice received unilateral cervical injection of rAAV2-retro-H2B-mGreenLantern virus. Two weeks later, brains were optically cleared by the 3DISCO method and were imaged using light-sheet microscopy. The image is viewed from the dorsal surface of the brain. Three distinct groups of cortico-spinal neurons (M1, RFA/2° Motor, 2° Sensory) are apparent; in diencephalon, hypothalamic-spinal neuronal nuclei. In midbrain, several populations of neurons are revealed such as red nucleus (RN), midbrain reticular neurons (MRN), Edinger Westhhal nucleus (Ewcp), and interstitial nucleus of Cajal (INC), among others. Scale bar, 0.5 mm.

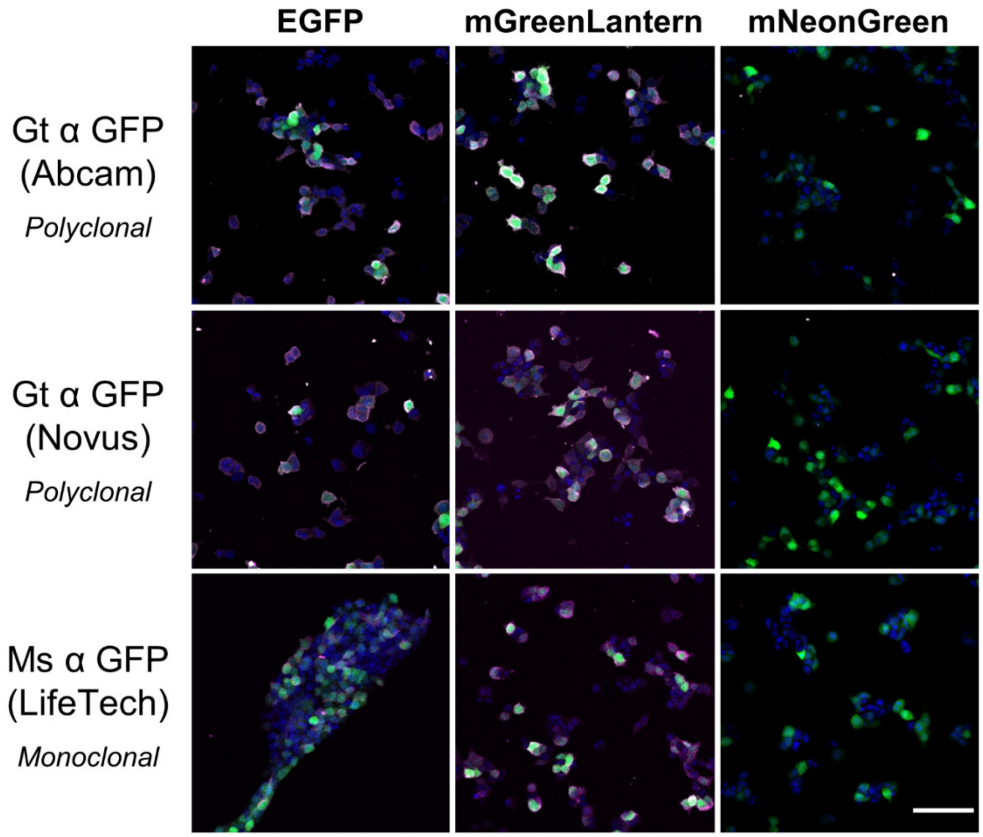

Fig. S3. mGreenLantern is compatible with commercially available EGFP antibodies. HEK293T cells were chemically transfected with an FP (green) and then immunostained using the indicated primary antibodies and the species-appropriate Alexa^{555}-conjugated secondary antibody (magenta), with DAPI staining (blue) to confirm the presence of cells. mNeonGreen is derived from *B. lanceolatum* rather than *A. victoria* and therefore serves as a negative control. Magnification, 4×. Scale bar, 100 µm.

A

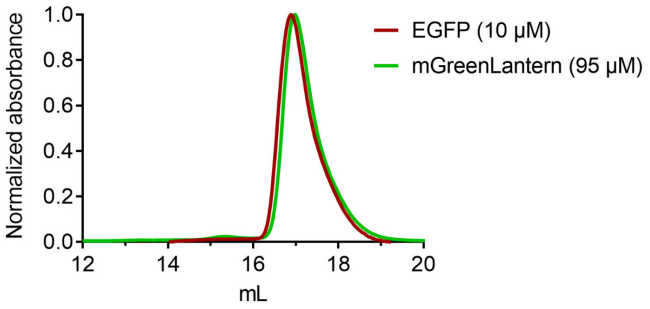

B

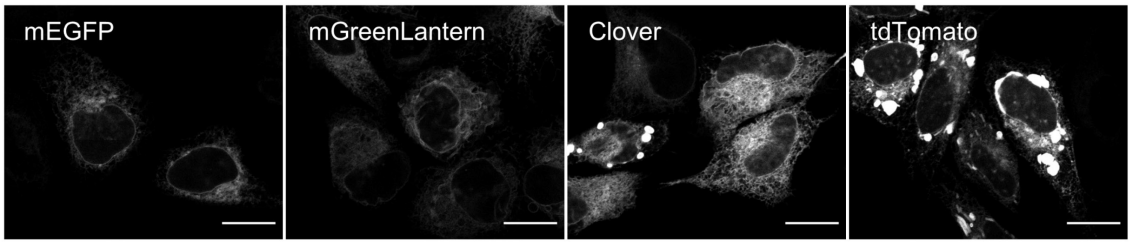

C

Fluorescent protein	# cells counted	# OSER	% normal cells	Interpretation
mEGFP (A206K)	141	20	86%	Monomer
mGreenLantern	231	30	86%	Monomer
Clover	233	68	71%	Weak dimer
tdTomato	207	148	29%	Dimer

Fig. S4. Oligomeric state of FPs. *(A)* Gel filtration chromatography of purified protein. mGreenLantern still eluted as a monomer at the high concentration of 95 µM. *(B)* Representative images of HeLa cells 16 hr after transfection with plasmids encoding CytERM-FP fusions for the organized smooth endoplasmic reticulum (OSER) assay. mEGFP and tandem dimer Tomato (tdTomato) are established monomers and dimers in this assay, respectively. Scale bars: 20 µm. *(C)* Quantitation of normal cells and cells containing OSER structures, for the FPs in *B*, according to criteria described in Costantini et al., *Traffic*, 2012.

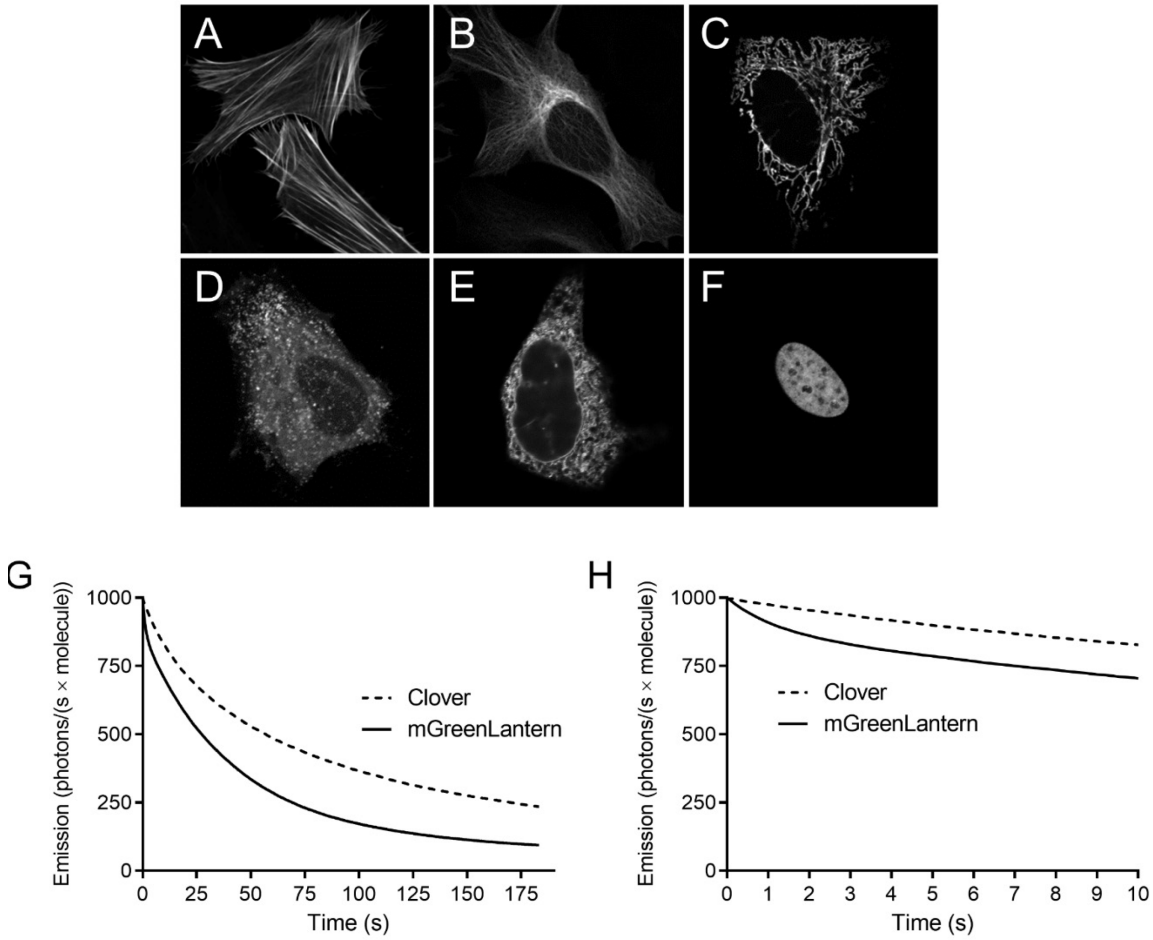

Fig. S5. Localization of fusion constructs and photostability in cells. (*A-F*) HeLa cells transfected with plasmids encoding: (*A*) LifeAct-7aa-mGreenLantern; actin. (*B*) mGreenLantern-6aa-tubulin; tubulin. (*C*) COX8A[×4]-4aa-mGreenLantern; mitochondria. (*D*) mGreenLantern-15aa-clathrin; clathrin. (*E*) Calreticulin-3aa-mGreenLantern-2aa-KDEL; endoplasmic reticulum. (*F*) H2B-6aa-mGreenLantern; nucleus. Plasmids are described further in Table S4. (*G*) Laser-scanning confocal microscopy photobleaching curves. The time axis is normalized to an initial scan-averaged emission rate of 1000 photons/s per molecule. (*H*) After a brief Emerald-like fast-bleaching component at the onset of high-intensity illumination (<20% of initial emission), mGreenLantern assumes a mono-exponential decay curve typical of GFPs.

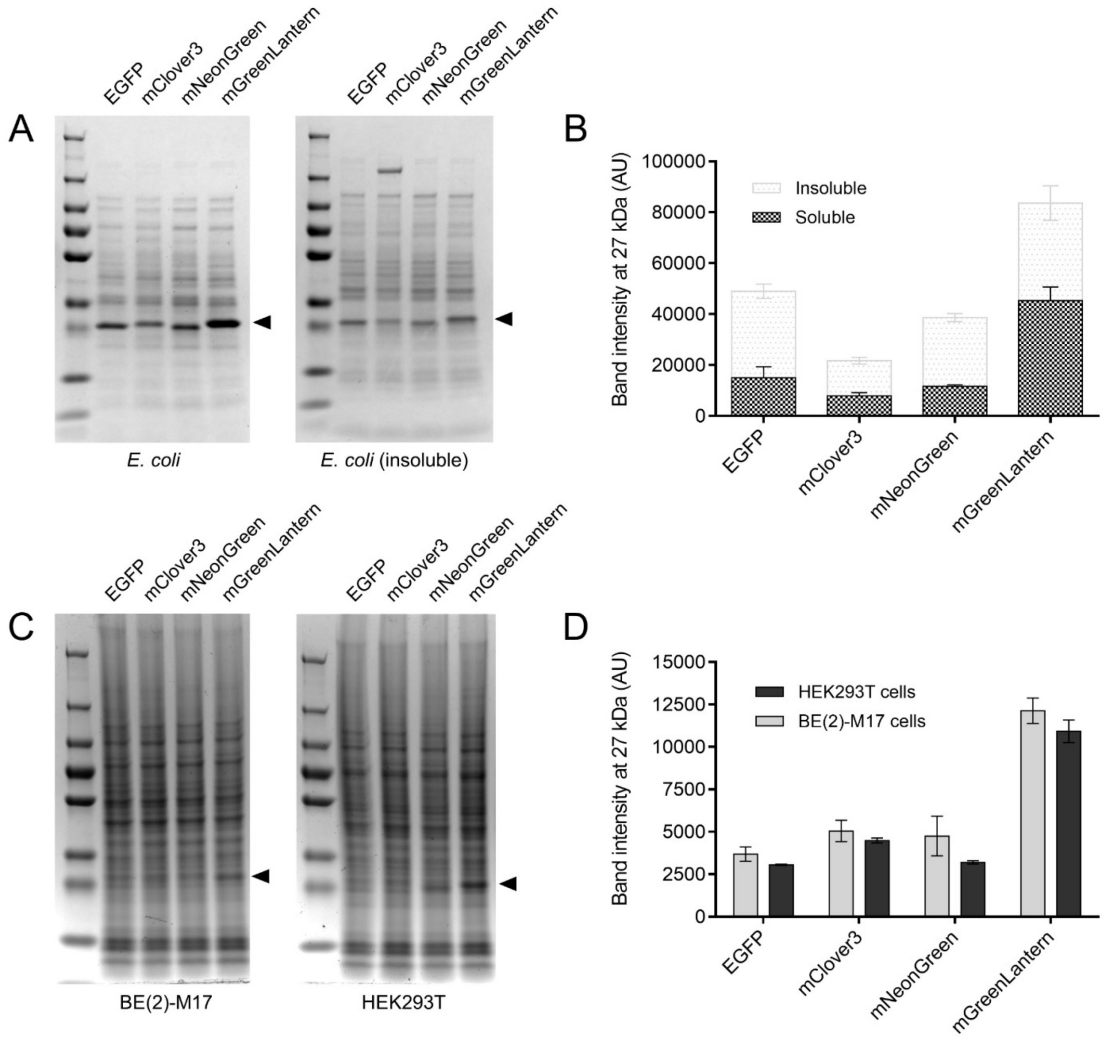

Fig. S6. Solubility of fluorescent proteins in bacterial and mammalian cells. Under matched experimental conditions, cells expressed more mGreenLantern protein than EGFP, mClover3, and mNeonGreen. (*A*) Representative Coomassie gels of soluble and insoluble protein fractions from *E. coli* lysate. Black arrowheads indicate the fluorescent protein band at ~27 kDa. *(B)* Band intensity of the gels was quantified using ImageJ by densitometry and displayed as a stacked bar graph, with total bar height representing the sum of soluble and insoluble protein fractions. *(C)* Coomassie gels of soluble protein extracted from BE(2)-M17 and HEK293T cells and *(D)* quantification of the gels from *C*. Mean ± SEM, n = 2 and n = 3 experimental replicates are presented in *B* and *D*, respectively.

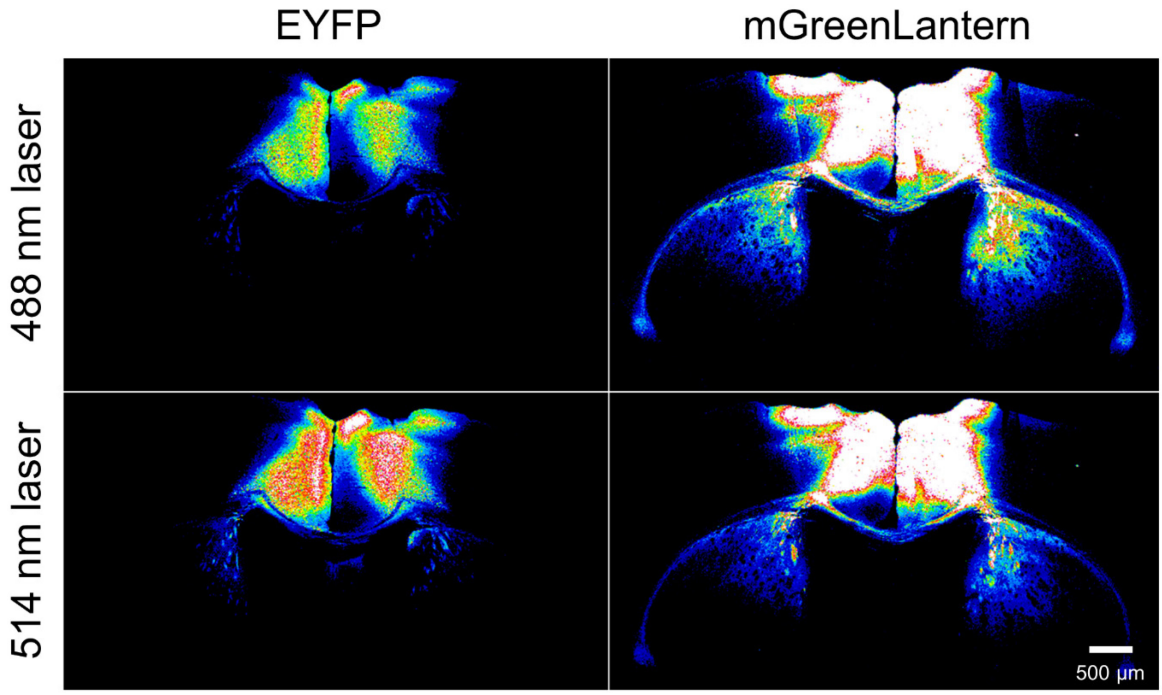

Fig. S7. Visibility of long-range projections was not due to specific laser selection. Intensity is represented using a 16-color lookup table from ImageJ. Sections were imaged 14 days after injecting AAV2/1-EF1α-DIO-[FP]-WPRE-pA virus into the anterior cingulate area (ACA), as in Fig. 2D-E. Magnification, 10×.

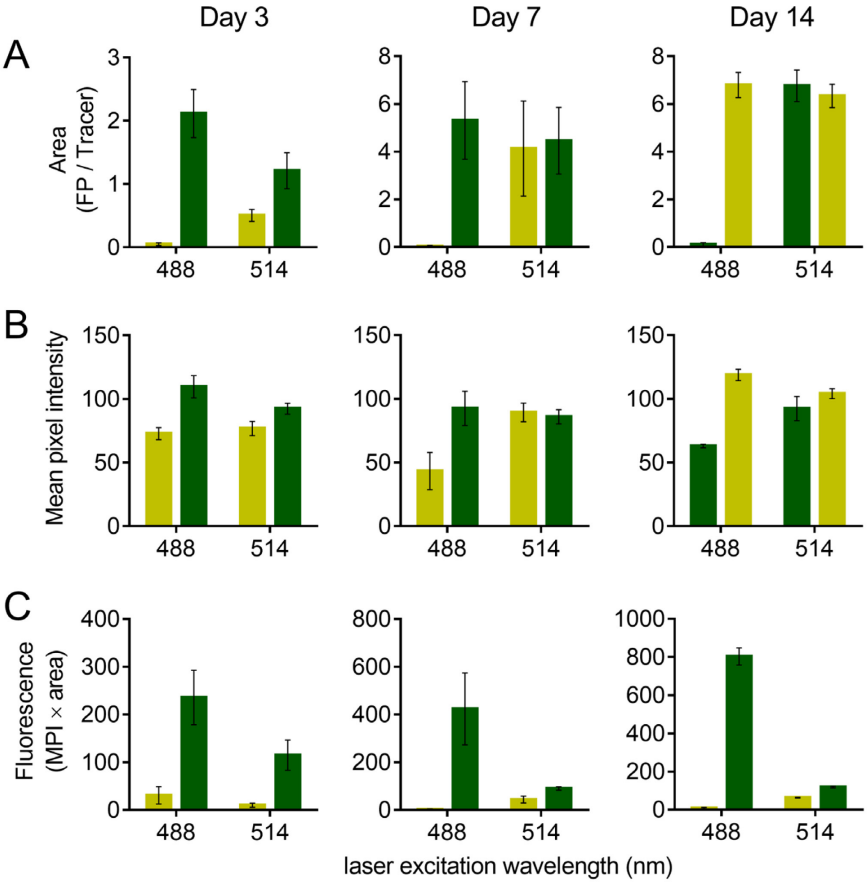

Fig. S8. Quantitation of images presented in Fig. 3B to estimate the *in vivo* fluorescent protein expression kinetics. (*A*) Area of ACA displaying FP signal, normalized to the full tracer area. (*B*) Mean pixel intensity of FP signal within the tracer area. (*C*) "Fluorescence" is the product of mean pixel intensity and area (defined in Fig. 3A). Mean ± SEM, n = 2 hemispheres per FP per time point.

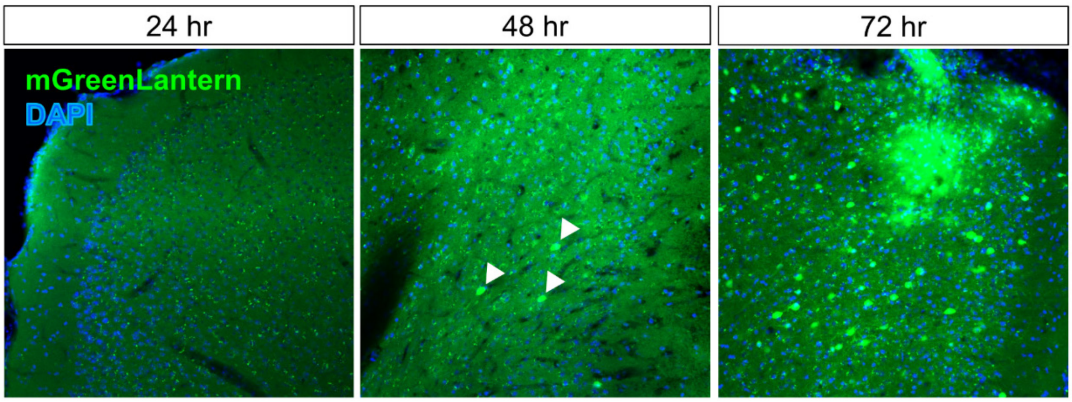

Fig. S9. mGreenLantern expressed rapidly in transgenic animals. The earliest signs of fluorescence were visible in cells bodies of parvalbumin (PV)-containing interneurons 48 hr after mice were injected with AAV2/1-EF1α-DIO-mGreenLantern-WPRE-pA virus into the anterior cingulate area (ACA) of PV-Cre mice. Cell bodies at the 48 hr time point are indicated by white arrowheads. Magnification, 20×.

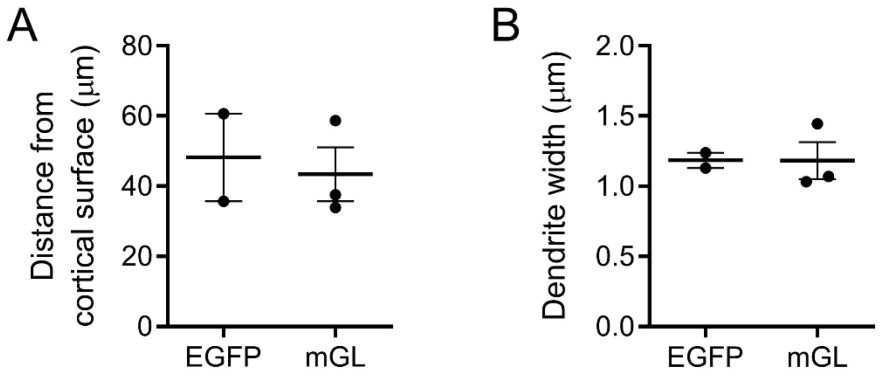

Fig. S10. Dendrites pictured in Fig. 4C and used for spine density measurements in Fig. 4D were of similar width and located a similar distance from the cortical surface. *(A)* Distance of quantified dendrites from the cortical surface per animal, mean ± SD. *(B)* Three separate width measurements from each dendrite were averaged and plotted for each animal, mean ± SEM.

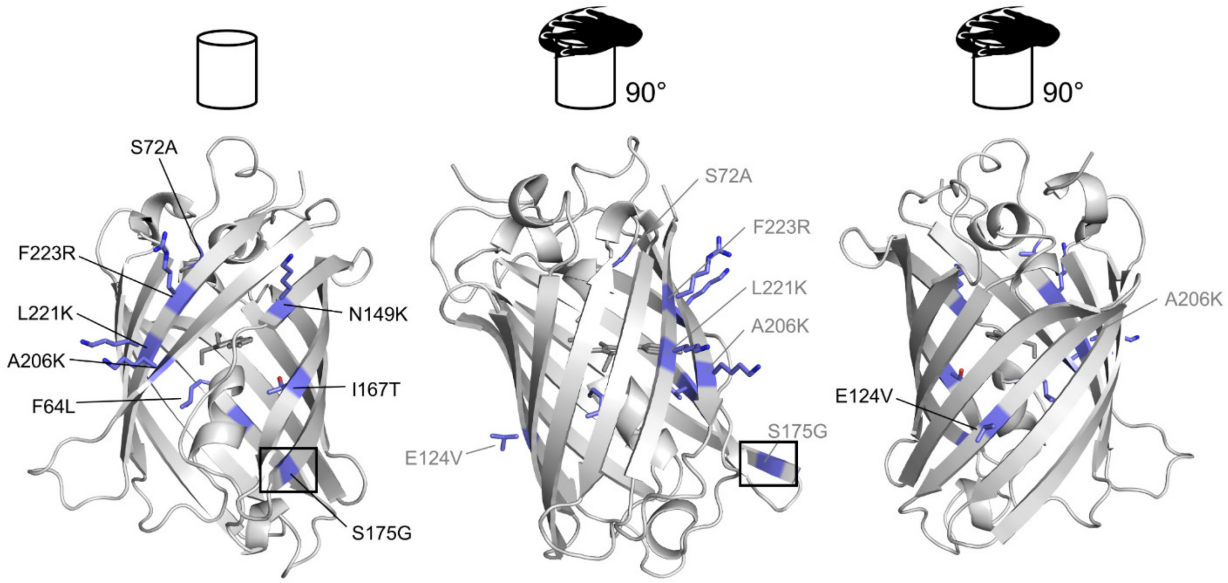

Fig. S11. Location of the mutations in mGreenLantern relative to Clover. Side chain orientations were manually selected using the PyMOL mutagenesis tool (not a homology model) to indicate the location of each mGL mutation relative to the Clover structure (PDB: 5WJ2). Residues that are labeled more than once, to assist with orientation, are greyed. The chromophore is colored grey inside the barrel, with the phenolate pointing toward β-strand 7 (same strand as position 149), most easily viewed in the first projection. Follow S175G to see first 90° counterclockwise rotation from the lid clearly (black box, to aid visual tracking). G232D is in a disordered region of the Clover structure C-terminus and is not pictured.

Table S1. Spectroscopic characterization and performance of FPs in cells.

Protein [a]	λ_{ex}	λ_{em}	ϕ	ε	Molecular brightness[b]	pK_a	**Cellular brightness**[c]			Maturation (min)
							HeLa	BE(2)-M17	HEK 293T	
EGFP	488	507	0.71 ± 0.010	53,400 ± 700	38.1	6.0 ± 0.19	1.0	1.0	1.1	28.0 ± 1.0
Superfolder GFP	485	508	0.67 ± 0.023	51,300 ± 1,400	34.2	6.2 ± 0.12	1.7	1.5	1.7	37.5 ± 5.8
Clover	505	515	0.75 ± 0.048	96,600 ± 1,400	72.3	6.5 ± 0.21	1.5	2.2	1.8	14.8 ± 0.3
mClover3	506	516	0.80 ± 0.015	100,000 ± 2,800	79.7	6.1 ± 0.02	2.4	2.1	1.6	36.5 ± 0.9
mNeonGreen	506	516	0.78 ± 0.037	115,400 ± 2,200	89.5	5.6 ± 0.25	3.2	3.3	4.1	18.0 ± 1.7
EYFP	513	527	0.62 ± 0.055	94,100 ± 2,800	58.2	6.8 ± 0.29	1.7	1.8	1.9	33.0 ± 1.4
FOLD1	503	514	0.70 ± 0.016	99,700 ± 2,000	69.9	5.8 ± 0.14	3.3	3.6	3.4	N.D. N.D.
mFOLD1	503	514	N.D. N.D.	N.D. N.D.	N.D.	5.9 ± 0.12	3.2	3.3	4.0	N.D. N.D.
mF1Y	503	517	N.D. N.D.	104,600 ± 570	77.4	N.D. N.D.	3.5	3.5	3.9	7.2 ± 0.8
mF1VPK	503	513	0.75 ± 0.013	107,700 ± 3,200	80.5	N.D. N.D.	3.1	3.6	3.2	N.D. N.D.
mF2BK (DMD)	503	514	0.71 ± 0.029	101,300 ± 2,700	71.6	5.6 ± 0.16	3.0	3.0	3.1	8.5 ± 0.5
mGreenLantern	503	514	0.72 ± 0.017	101,800 ± 630	73.6	5.6 ± 0.01	6.2	6.3	7.4	13.5 ± 1.5
mF2BK-K (DMN)	502	514	N.D. N.D.	N.D. N.D.	N.D.	N.D. N.D.	2.9	2.9	3.3	N.D. N.D.
mF3CPK	503	513	0.72 ± 0.014	100,700 ± 4,500	72.6	5.9 ± 0.27	2.3	2.6	2.4	N.D. N.D.

[a] All values reported here were generated in our lab for this study ($n \geq 3$ replicate experiments each). For ϕ, ε, pK_a, and maturation data, the mean and standard deviation are in the left and right columns, respectively.

[b] Molecular brightness = $(\phi \times \varepsilon)/10^3$, where ϕ is quantum yield and ε is extinction coefficient (M^{-1} cm^{-1}) at the absorbance peak.

[c] Fold brightness in the specified cell line relative to EGFP.

Table S2. Mutations present in each Clover variant described in this study.

Clover [a] →	A206	E124	G232	D234	K101	T105	S147	L221	F223	N149	G4	Brightness in HeLa cells
FOLD1	-	-	-	-	-	-	-	-	-	-	-	3.3
mFOLD1	K	-	-	-	-	-	-	-	-	-	-	3.2
mF1Y	K	-	-	-	-	-	-	-	-	Y	-	3.5
mF1VPK	K	V	-	-	-	-	P	-	-	K	-	3.1
F2B	V	V	D	-	-	-	-	-	-	-	-	N.D.
mF2B	V	V	D	-	-	-	-	K	R	-	-	N.D.
mF2B-ΔG	V	V	D	-	-	-	-	K	R	-	Δ	N.D.
mF2BK	V	V	D	-	-	-	-	K	R	K	-	3.0
mGreenLantern	K	V	D	-	-	-	-	K	R	K	-	6.2
mF2BKK (DMN)	K	V	D	N	-	-	-	K	R	K	-	2.9
mF2B2	V	V	D	N	-	-	-	K	R	-	-	N.D.
F3C	V	V	D	N	E	Y	-	-	-	-	-	N.D.
F3CP	V	V	D	N	E	Y	P	-	-	-	-	N.D.
mF3CP	V	V	D	-	E	Y	P	K	R	-	-	N.D.
mF3CPK	V	V	D	-	E	Y	P	K	R	K	-	2.3
mF3CPK-ΔG	V	V	D	-	E	Y	P	K	R	K	Δ	N.D.

[a] All FPs in the table, except Clover, additionally carry F64L/S72A/I167T/S175G mutations (not displayed in table). To facilitate sequence comparison, mutated sites in column headers are not listed in numerical order.

Δ Deleted residue.

Table S3. Fluorescent protein amino acid sequence alignment.

```
                1         10        20        30        40        50
                |         |         |         |         |         |
EGFP            MVSKGEELFTGVVPILVELDGDVNGHKFSVSGEGEGDATYGKLTLKFICTTGKLPVPWPT
sfGFP           MVSKGEELFTGVVPILVELDGDVNGHKFSVRGEGEGDATNGKLTLKFICTTGKLPVPWPT
Clover          MVSKGEELFTGVVPILVELDGDVNGHKFSVRGEGEGDATNGKLTLKFICTTGKLPVPWPT
mGL             MVSKGEELFTGVVPILVELDGDVNGHKFSVRGEGEGDATNGKLTLKFICTTGKLPVPWPT

                60        70        80        90        100       110
                |         |         |         |         |         |
EGFP            LVTTLTYGVQCFSRYPDHMKQHDFFKSAMPEGYVQERTIFFKDDGNYKTRAEVKFEGDTL
sfGFP           LVTTLTYGVQCFSRYPDHMKRHDFFKSAMPEGYVQERTISFKDDGTYKTRAEVKFEGDTL
Clover          LVTTFGYGVACFSRYPDHMKQHDFFKSAMPEGYVQERTISFKDDGTYKTRAEVKFEGDTL
mGL             LVTTLGYGVACFARYPDHMKQHDFFKSAMPEGYVQERTISFKDDGTYKTRAEVKFEGDTL

                120       130       140       150       160       170
                |         |         |         |         |         |
EGFP            VNRIELKGIDFKEDGNILGHKLEYNYNSHNVYIMADKQKNGIKVNFKIRHNIEDGSVQLA
sfGFP           VNRIELKGIDFKEDGNILGHKLEYNFNSHNVYITADKQKNGIKANFKIRHNVEDGSVQLA
Clover          VNRIELKGIDFKEDGNILGHKLEYNFNSHNVYITADKQKNGIKANFKIRHNVEDGSVQLA
mGL             VNRIVLKGIDFKEDGNILGHKLEYNFNSHKVYITADKQKNGIKANFKTRHNVEDGGVQLA

                180       190       200       210       220       230
                |         |         |         |         |         |
EGFP            DHYQQNTPIGDGPVLLPDNHYLSTQSALSKDPNEKRDHMVLLEFVTAAGITLGMDELYK
sfGFP           DHYQQNTPIGDGPVLLPDNHYLSTQSVLSKDPNEKRDHMVLLEFVTAAGITHGMDELYK
Clover          DHYQQNTPIGDGPVLLPDNHYLSHQSALSKDPNEKRDHMVLLEFVTAAGITHGMDELYK
mGL             DHYQQNTPIGDGPVLLPDNHYLSHQSKLSKDPNEKRDHMVLKERVTAAGITHDMDELYK
```

Bold: differences relative to EGFP.
Magenta: chromophore tripeptide.
Green: differences between mGreenLantern (mGL) and Clover.

Note: Q80R and L231H are regarded as neutral.

Table S4. Sources of plasmid backbones used for cloning mGreenLantern and construction of targeting vectors and virus.

Plasmid backbone templates	Addgene #	Depositor	Reference
pBAD-LSSmOrange	37129	Vladislav Verkhusha	(9)
pcDNA3.1.1-Clover-mRuby2	49089	Kurt Beam	*unpublished*
pcDNA-4mtD3cpv	36324	Amy Palmer & Roger Tsien	(10)
YPet-H2B-6	56632	Michael Davidson	*unpublished*
pLifeAct-mTurquoise2	36201	Dorus Gadella	(11)
EGFP-Tubulin-6	56450	Michael Davidson	(12)
mAmetrine-Clathrin-15	56542	Michael Davidson	*unpublished*
AmCyan-P2A-mCherry	45350	Ilpo Huhtaniemi	(13)
pAAV-EF1a-DIO EYFP	27056	Karl Deisseroth	*unpublished*
pAAV-CAG-GFP	37825	Edward Boyden	*unpublished*

Movie S1. 3D visualization of supraspinal projection neuron nuclei expressing mGreenLantern. Adult mice received a unilateral cervical injection of rAAV2-retro-mGreenLantern (see "Spinal cord surgery" in Methods). Two weeks later, brains were optically cleared by the 3DISCO method and imaged using light-sheet microscopy. The video illustrates the overall distribution of spinal cord projection neurons.

SI References

1. D. G. Gibson, Enzymatic Assembly of Overlapping DNA Fragments. *Methods Enzymol.* **498**, 349–361 (2011).

2. S. Pletnev, *et al.*, Orange fluorescent proteins: Structural studies of LSSmOrange, PSmOrange and PSmOrange2. *PLoS One* **9**, 1–12 (2014).

3. J. Quan, J. Tian, Circular polymerase extension cloning. *Nat. Protoc.* **6**, 242–251 (2011).

4. D. J. Korbie, J. S. Mattick, Touchdown PCR for increased specificity and sensitivity in PCR amplification. *Nat. Protoc.* **3**, 1452–1456 (2008).

5. B. C. Campbell, G. A. Petsko, C. F. Liu, Crystal Structure of Green Fluorescent Protein Clover and Design of Clover-Based Redox Sensors. *Structure* **26**, 225-237.e3 (2018).

6. P. J. Cranfill, *et al.*, Quantitative assessment of fluorescent proteins. *Nat. Methods* **13**, 557–562 (2016).

7. C. Soderblom, *et al.*, 3D Imaging of Axons in Transparent Spinal Cords from Rodents and Nonhuman Primates. *eNeuro* **2**, ENEURO.0001-15.2015 (2015).

8. Z. Wang, B. Maunze, Y. Wang, P. Tsoulfas, M. G. Blackmore, Global Connectivity and Function of Descending Spinal Input Revealed by 3D Microscopy and Retrograde Transduction. *J. Neurosci.* **38**, 10566 LP – 10581 (2018).

9. D. M. Shcherbakova, M. A. Hink, L. Joosen, T. W. J. Gadella, V. V Verkhusha, An Orange Fluorescent Protein with a Large Stokes Shift for Single-Excitation Multicolor FCCS and FRET Imaging. *J. Am. Chem. Soc.* (2012).

10. A. E. Palmer, *et al.*, Ca2+ Indicators Based on Computationally Redesigned Calmodulin-Peptide Pairs. *Chem. Biol.* **13**, 521–530 (2006).

11. J. Goedhart, *et al.*, Structure-guided evolution of cyan fluorescent proteins towards a quantum yield of 93%. *Nat. Commun.* **3**, 751 (2012).

12. M. A. Rizzo, M. W. Davidson, D. W. Piston, Fluorescent protein tracking and detection: Fluorescent protein structure and color variants. *Cold Spring Harb. Protoc.* (2009) https:/doi.org/10.1101/pdb.top63.

13. I. Potorac, *et al.*, A vital region for human glycoprotein hormone trafficking revealed by an LHB mutation. *J. Endocrinol.* (2016) https:/doi.org/10.1530/JOE-16-0384.